The shape of soap films and Plateau borders

2007 J. Phys.: Condens. Matter 19 246106

(http://iopscience.iop.org/0953-8984/19/24/246106)

IOP PUBLISHING JOURNAL OF PHYSICS: CONDENSED MATTER

J. Phys.: Condens. Matter **19** (2007) 246106 (13pp) doi:10.1088/0953-8984/19/24/246106

The shape of soap films and Plateau borders*

M A Fortes[1], P I C Teixeira[2,3] and A M Deus[1]

[1] Departamento de Engenharia de Materiais and Instituto de Ciência e Engenharia de Materiais e Superfícies, Instituto Superior Técnico, Avenida Rovisco Pais, P-1049-001 Lisbon, Portugal
[2] Instituto Superior de Engenharia de Lisboa Rua Conselheiro Emídio Navarro 1, P-1950-062 Lisbon, Portugal
[3] Centro de Física Teórica e Computacional, Universidade de Lisboa, Avenida Professor Gama Pinto 2, P-1649-003 Lisbon, Portugal

Received 24 November 2006, in final form 18 April 2007
Published 22 May 2007
Online at stacks.iop.org/JPhysCM/19/246106

Abstract

We have calculated the shapes of flat liquid films, and of the transition region to the associated Plateau borders (PBs), by integrating the Laplace equation with a position-dependent surface tension $\gamma(x)$, where $2x$ is the local film thickness. We discuss films in either zero or non-zero gravity, using standard $\gamma(x)$ potentials for the interaction between the two bounding surfaces. We have investigated the effects of the film flatness, liquid underpressure, and gravity on the shape of films and their PBs. Films may exhibit 'humps' and/or 'dips' associated with inflection points and minima of the film thickness. Finally, we propose an asymptotic analytical solution for the film width profile.

1. Introduction

Free liquid films (e.g. soap films) terminate at Plateau borders (PBs), where they contact a confining wall (a solid wall or a liquid pool, see figures 1(a) and (b), respectively) or other films (see figure 1(c)). In the bulk of a fairly dry liquid foam, three films meet at a PB, which therefore has a triangular cross-section; the PBs themselves meet in fours at quadruple junctions, or nodes. The identification of films, PBs and quadruple junctions is somewhat arbitrary, particularly in a fairly wet foam, since there is no sharp transition from one to the other, but is nevertheless very convenient for the description and analysis of foam phenomena. In line with this identification, a (uniform) film tension γ_F is usually assigned to the film (of uniform thickness, often taken to be zero), while the tension of the surfaces of PBs and quadruple junctions is taken to be γ_L, the bulk liquid surface tension. It is often assumed that $\gamma_F = 2\gamma_L$, implying that the PB surfaces join the film tangentially, as shown in figure 1(d). In fact, the film tension γ_F depends on the film thickness, $2x$, because the two film surfaces interact: therefore γ_F changes from point to point in a film of non-uniform thickness, which is necessarily the case in the film–PB transition region. In what follows we sometimes refer

* This paper is dedicated to the memory of Professor Manuel Amaral Fortes, who passed away on April 22nd 2007.

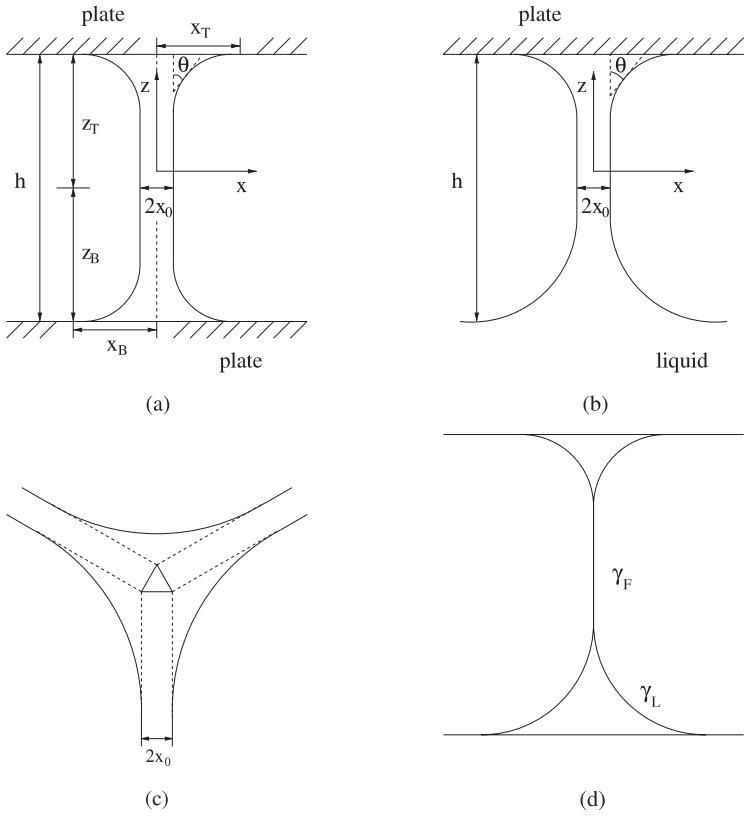

Figure 1. (a) Vertical planar film between two plates. (b) Vertical planar film between a top plate and a pool of liquid at the bottom: x_0 is the film width at the neck and θ is the slope of the film surface. (c) Symmetrical triple film junction. (d) Idealized thin film with PBs: γ_F is the film tension; $\gamma_L = \gamma_F/2$ is the bulk liquid tension. In all cases the film is unbounded in the y direction, perpendicular to the plane of the page.

to the film including PBs as the 'whole film', and to the film excluding PBs (i.e., to what is conventionally known as 'film') as the 'conventional film'.

The purpose of this paper is to determine the shape of a free liquid film and associated PBs, taking into account the thickness dependence of the interaction between the two surfaces bounding the film and its PBs. This we do by assigning a surface tension $\gamma(x)$, where $2x$ is the film thickness, to each surface. The film tension $\gamma_F(x)$ then equals $2\gamma(x)$. We investigate only 'flat' films, i.e., those with a mid-plane of mirror symmetry: they are uniform along the third dimension; such films are connected to PBs, hence must have a neck of thickness $2x_0$. For such films the equilibrium Laplace equation with a position-dependent $\gamma(x)$ can be integrated by standard numerical methods. Extension to, e.g., axially symmetric films, or films of arbitrary constant curvature as in a foam at equilibrium, where the two surfaces bounding the film are not mirror images, is a much more complicated undertaking. We start by discussing gravity-free films between two plates (figure 1(a)), and then investigate the effect of gravity on vertical films either between two plates, or between a plate and a pool (figure 1(b)).

Recently Starov [1] has performed a semi-quantitative analysis of the shapes of gravity-free thin films on a solid substrate using an equation originally proposed by Derjaguin [2, 3] (and often referred to as Derjaguin's equation). In particular, Starov investigated the transition

regions from films to cylindrically symmetric liquid drops and menisci on plates and capillaries, for given liquid–solid contact angles. Various types of features were identified and their relative stability assessed through free energy calculations. In the present paper we carry out a similar study of free liquid films with a mid-plane of symmetry, on the basis of a different equation for the film profile, which we numerically integrate. The film tension is assumed to be thickness dependent and gravity is included. We also derive an asymptotic solution to this equation around the film neck.

This paper is organized as follows: in section 2 we introduce a model for the interaction $\gamma(x)$ between film surfaces. Next, in section 3 we derive the Laplace equation for a planar film endowed with this $\gamma(x)$, which is non-dimensionalized and numerically integrated, for films in zero and non-zero gravity, in section 4. In section 5 we discuss, on a semi-quantitative level, the relationship between $\gamma(x)$ and features of the film shape. Then in section 6 we obtain an approximate (asymptotic) solution to the Laplace equation for the conventional film and compare it with those found numerically in the preceding section. Finally, our results are summarized in section 7. Technical details pertaining to the solution of the film shape equation are collected in the appendix.

2. Interaction between film surfaces

The main contributions to the energy per unit area $\gamma_{\mathrm{F}} = 2\gamma(x)$ of a flat, aqueous soap film of uniform thickness $2x$ stabilized by ionic surfactants include a van der Waals attraction, a double-layer repulsion, and a short-range, Born-type repulsion (see [4, 5], and references therein). There is evidence [6–8] that $\gamma(x)$ may have more than one minimum, as in figure 2. These considerations also apply to liquid films on solid substrates. A soap film whose thickness is close to the first minimum (the smaller x_{M}, typically of the order of 4 nm) is called a Newton black film; if its thickness is instead close to the second minimum (the larger x_{M}, typically of the order of 50 nm), it is known as a common black film [5]. It has been suggested [6] that other minima may exist which are associated with thicker films (figure 2(c)). There is no consensus in the literature on the exact form of $\gamma(x)$ except with regard to the van der Waals attraction, which is $A_{\mathrm{H}}/(48\pi x^2)$ with A_{H} the Hamaker constant (recall that x is *half* the film thickness).

Stable flat (uniform-thickness, zero-curvature) films can exist if their thickness $2x$ is such that $\partial\gamma/\partial x < 0$ and $\partial^2\gamma/\partial x^2 > 0$ [3]. The pressure

$$\pi = -\frac{\partial\gamma}{\partial x} = -\frac{\partial\gamma_{\mathrm{F}}}{\partial(2x)}, \tag{1}$$

is usually called the *disjoining pressure*, a term introduced by Derjaguin [9]. This quantity is experimentally accessible (see, e.g., [5]); typical values are in the range 50 Pa–50 kPa [6]. In our calculations we shall use the following form for $\gamma(x)$ [4, 10]:

$$\gamma(x) = \gamma_{\mathrm{L}} + \frac{b_1}{x^n} - \frac{b_2}{x^2} + b_3\exp(-b_4 x), \tag{2}$$

where n and b_i ($i = 1, 2, 3, 4$) are constants chosen such that $\gamma(x)$ (and thus also $\pi(x)$; see section 3) has two minima. Here the b_1 term models the steep Born repulsion, the b_2 term is the Van der Waals interaction, and the exponential term is a double-layer repulsion of strength b_3 and inverse screening length b_4. As required, $\gamma(x)$ approaches γ_{L} on increasing x (i.e. on approaching a PB). Equation (2) is sufficiently general to describe films made from either ionic or non-ionic surfactants, depending on b_3/b_2; effects such as micelle formation have been neglected at this stage. Figures 2(a) and (b) plot $\gamma(x)$ and $\pi(x)$ for potential A in table 1: they have the same shape and both tend to a constant value (γ_{L} or 0, respectively) at large x, and to

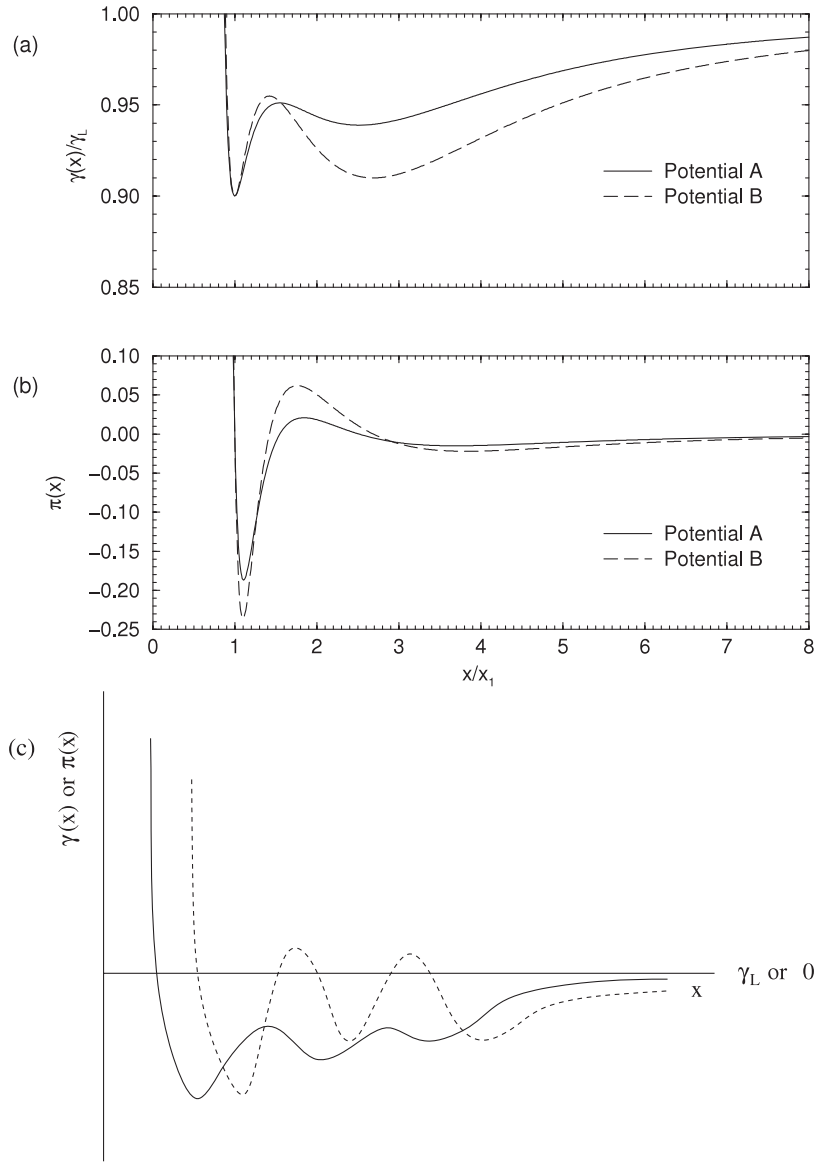

Figure 2. (a) Interaction potential $\gamma(X)$, equation (16), and (b) disjoining pressure $\pi(X) = -\mathrm{d}\gamma(x)/\mathrm{d}x$, for potentials A (solid lines) and B (dashed lines) in table 1. The parameters are chosen so that the potential has a realistic shape with a deep first minimum and a shallower second minimum; see, e.g., [5]. (c) Schematic representation of a possible $\gamma(x)$ (solid line) and $\pi(x)$ (dashed line) with more than two minima [6].

infinity as $x \to 0$, going through two minima. Equation (2) can also describe the two outermost minima of a potential with more than two minima.

3. Laplace equation for a film with a mid-plane of mirror symmetry and thickness-dependent surface energy

We take the yz-plane to lie in the mid-plane of mirror symmetry of the film, with the vertical z-axis directed upwards (see figure 1). The film is unbounded in the (horizontal) y-direction,

Table 1. Parameters of the interaction potentials, equation (16) (see the text for details). The two minima are at $X_1 = 1$ and X_2 and have depths $\Gamma(X_1) = 0.9$ and $\Gamma(X_2)$, respectively.

Potential	B_1	B_2	B_3	B_4	X_2	$\Gamma(X_2)$
A	0.053 4695	0.822 860	3.0	1.5	2.515 834	0.938 893
B	0.075 7825	1.291 430	5.0	1.5	2.689 082	0.909 958

but confined in the z-direction by two horizontal walls a distance h apart, say at $z = 0$ and $z = h$ (the bottom wall can be a liquid pool). The x-coordinate ($x > 0$) is the distance from the yz-mid-plane to the film surfaces; the (whole) film profile (i.e. including the PB) is given by $x(z)$, and its width at the neck (where $\dot{x} = \mathrm{d}x/\mathrm{d}z = 0$) is $2x_0$.

The free energy E of the whole film (including PBs) per unit length along y comprises the surface energy and the gravitational potential energy; taking, for the moment, $z = 0$ at the bottom wall (where we define the gravitational potential energy to be zero), we have

$$\frac{E}{2} = \int_0^h \gamma(x)(1+\dot{x}^2)^{1/2}\,\mathrm{d}z + \rho_{\mathrm{L}} g \int_0^h xz\,\mathrm{d}z, \tag{3}$$

where ρ_{L} is the liquid density, g is the acceleration of gravity, and the dot denotes differentiation with respect to z. The volume of liquid per unit length in the y-direction (i.e. the area A enclosed by the profile $x(z)$) is

$$\frac{A}{2} = \int_0^h x\,\mathrm{d}z. \tag{4}$$

The equilibrium condition is that E be minimized at fixed A. Introducing a Lagrange multiplier π_0, this implies

$$\delta\left\{\int_0^h [\gamma(x)(1+\dot{x}^2)^{1/2} + \rho_{\mathrm{L}} g x z + \pi_0 x]\,\mathrm{d}z\right\} \equiv \delta\left[\int_0^h F(x,\dot{x},z)\right] = 0. \tag{5}$$

The corresponding Euler–Lagrange equation is

$$\frac{\mathrm{d}}{\mathrm{d}z}\left(\frac{\partial F}{\partial \dot{x}}\right) - \frac{\partial F}{\partial x} = 0, \tag{6}$$

leading to the Laplace equation for a film with position-dependent γ:

$$\frac{\mathrm{d}}{\mathrm{d}z}\left[\gamma(x)\frac{\dot{x}}{\left(1+\dot{x}^2\right)^{1/2}}\right] - (1+\dot{x}^2)^{1/2}\frac{\mathrm{d}\gamma}{\mathrm{d}x} = \pi_0 + \rho_{\mathrm{L}} g z. \tag{7}$$

This equation was derived previously by Fortes [11], who showed that its form does not depend on the wettability of the confining solid surfaces: this only enters through the boundary conditions. A similar equation has been recently proposed by Starov [1], who attributed it to Derjaguin. Unlike Derjaguin's, equation (7) includes both a thickness-dependent surface tension $\gamma(x)$ and gravity.

The radius of curvature $r(x)$ of the film surface $x(z)$ ($r(x) > 0$ if the centre of curvature is outside the film and $r(x) < 0$ otherwise) is given by

$$\frac{1}{r(x)} = \frac{\ddot{x}}{(1+\dot{x}^2)^{3/2}} = \frac{\mathrm{d}}{\mathrm{d}z}\left[\frac{\dot{x}}{(1+\dot{x}^2)^{1/2}}\right], \tag{8}$$

and the angle $\theta \in [-\pi/2, \pi/2]$ defining the film surface slope relative to the z-axis (see figure 1(a)) is

$$\cos\theta = (1+\dot{x}^2)^{-1/2}. \tag{9}$$

(Note that $\cos\theta$ only takes positive values.) At the film neck, $\dot{x} = 0$ and $\theta = 0$. Using equations (8) and (9), equation (7) can be written in the form

$$\frac{\gamma(x)}{r(x)} - \cos\theta\,\frac{\mathrm{d}\gamma}{\mathrm{d}x} = \pi_0 + \rho_{\mathrm{L}} g z. \tag{10}$$

This equation can be interpreted in terms of an equilibrium of pressures: the pressure in the surrounding gas exceeds the pressure inside the liquid at z by $\Delta p = \pi_0 + \rho_{\mathrm{L}} g z$, where π_0 is the excess pressure at $z = 0$. We shall henceforth refer to π_0 as the *liquid underpressure*: it is balanced by the capillary pressure $\gamma(x)/r(x)$, which dominates at large x in the PB region; and by a disjoining pressure $-\cos\theta[\mathrm{d}\gamma(x)/\mathrm{d}x]$, which dominates at small x, in the nearly flat thin-film region (the conventional film). For constant γ, equations (7) and (10) reduce to the usual form of the Laplace equation for a vertical interface under gravity, which is invariant in the y direction. In particular, note that for $\gamma(x) \approx \gamma_{\mathrm{L}}$, as in the PB region, the radius r is approximately constant for $g = 0$ ($r = \gamma_{\mathrm{L}}/\pi_0$), i.e., the surface profile approaches a circle of radius $\pi_0/\gamma_{\mathrm{L}}$. Indeed, at the ends of a conventional gravity-free film of negligible thickness, the PB surfaces are usually taken to be circular.

Noting that

$$\frac{1}{r(x)} = \frac{\mathrm{d}(\sin\theta)}{\mathrm{d}z} = -\frac{\mathrm{d}(\cos\theta)}{\mathrm{d}x}, \tag{11}$$

and that

$$\frac{\mathrm{d}(\cos\theta)}{\mathrm{d}x} = -\ddot{x}\cos^3\theta, \tag{12}$$

equation (10) can be rewritten in the form

$$\ddot{x} = \frac{\pi_0 + \rho_{\mathrm{L}} g z - \pi(x)\cos\theta}{\gamma(x)\cos^3\theta}, \tag{13}$$

where $\cos\theta$ is given by equation (9) and we have used the fact that $\mathrm{d}[\gamma(x)]/\mathrm{d}x = -\pi(x)$. Equation (13) is the key equation of this paper.

4. Numerical integration of the Laplace equation

It is convenient to introduce non-dimensional quantities. We take as the unit of length the film half-thickness, x_1, at the first minimum of the potential $\gamma(x)$, and as the unit of surface energy per unit area the liquid surface tension γ_{L}, whence

$$X = \frac{x}{x_1}, \qquad Z = \frac{z}{x_1}, \qquad \Gamma(x) = \frac{\gamma(x)}{\gamma_{\mathrm{L}}}$$
$$\Pi_0 = \frac{x_1\pi_0}{\gamma_{\mathrm{L}}}, \qquad c^2 = \frac{\gamma_{\mathrm{L}}}{\rho_{\mathrm{L}} g}, \qquad G = \left(\frac{x_1}{c}\right)^2 = \frac{\rho_{\mathrm{L}} g}{\gamma_{\mathrm{L}}} x_1^2, \tag{14}$$

c being the capillary length of the (bulk) liquid; note that $G \propto g$, hence it is a measure of the strength of gravity. In terms of the reduced quantities given by equations (14), equation (13) becomes

$$\ddot{X} = \frac{\Pi_0 + GZ - \Pi(X)\cos\theta}{\Gamma(X)\cos^3\theta}, \tag{15}$$

where $\Pi(X) = \mathrm{d}\Gamma(X)/\mathrm{d}X$. We used a dimensionless interaction potential of the form of equation (2) with $n = 12$:

$$\Gamma(X) = 1 + \frac{B_1}{X^{12}} - \frac{B_2}{X^2} + B_3\exp(-B_4 X), \tag{16}$$

where $B_1 = b_1/\gamma_L x_1^{12}$, $B_2 = b_2/\gamma_L x_1^2$, $B_3 = b_3/\gamma_L$ and $B_4 = 1/x_1$ are determined by requiring that $\Gamma(X)$ have a minimum of depth Γ_1 at $X = 1$, i.e., $\Pi(X = 1) = 0$ and $\Gamma(X = 1) = \Gamma_1$, and in some cases a second minimum at $X > 1$. In the remainder of this paper we restrict ourselves to just a few sets of parameters, collected in table 1, that give $\Gamma(X)$ and $\Pi(X)$ of the general shape seen in experiments [5]; see figure 2. These sets of parameters were selected to illustrate different possible behaviours of the film profiles.

The procedure for integrating equation (15) is described in detail in the appendix. The boundary conditions appropriate to two completely wettable plates (or a completely wettable plate and a liquid pool) are that the angle θ, defining the slope of the film surface (see figures 1(a) and (b), respectively), should reach $\pi/2$ (top branch of film) or $-\pi/2$ (lower branch). Gravity-free films are calculated in the same manner: now $G = 0$ (no gravity) and the two branches are identical. For symmetrical film triple junctions, θ should reach $\pi/6$ (see figure 1(c)); we do not consider this case here.

Rather than X_0 we found it convenient to use as a parameter in our calculations the surface curvature $\ddot{X}$ at the film neck (where by definition $\dot{X} = 0$ and $\cos\theta = 1$), henceforth denoted by κ and given by (see equation (15))

$$\kappa = \frac{1}{\Gamma(X_0)}[\Pi_0 - \Pi(X_0)]. \tag{17}$$

For a given choice of interaction potential $\Gamma(X)$, calculation of a film profile proceeds as follows: we specify κ and Π_0, and if necessary G (vertical films). If $\Gamma(X)$ has more than one minimum, we also need to specify near which minimum we want X_0 to be. X_0 is then found by solving the non-linear algebraic equation (17). Once X_0 is known, equation (15) can be integrated by the method described in the appendix.

The effects of Π_0 and κ on gravity-free films are illustrated in figure 3 for potential A in table 1; here X_0 is close to the second minimum. Varying Π_0 at constant κ does not significantly change the length or thickness of the conventional film but impacts dramatically on PB (hence whole-film) size (as noted before, the radius of curvature of the PB is $1/\Pi_0$ for $G = 0$). On the other hand, for constant Π_0, the smaller κ, the flatter the film. Further decreasing κ would lead to longer films, but this is outside the reach of all numerical methods used (see the appendix).

We also looked at the experimentally relevant situation where the film geometry is changed at constant liquid volume, e.g., by varying the distance H between the bounding plates. In order to accomplish this, both Π_0 and κ need to be varied in concert. Results are shown in figure 4: on stretching a film its underpressure Π_0 remains nearly constant (and therefore so does the PB radius), but both its thickness X_0 and its curvature at the neck κ decrease substantially.

Finally the effect of gravity was investigated: in figure 5, film and PB profiles are plotted, for potential A in table 1, fixed Π_0 and κ and varying G (or g). If G is small, the larger G the more (top–bottom) asymmetric the film, as would be expected, and the more the PB surfaces deviate from circles. We also found that there is a limiting G^* above which there is no solution with $\ddot{X} > 0$ everywhere (i.e., there are 'dips' in the profile). For $G > G^*$ quite complex film shapes result: more and more dips appear, and the film can become either more or less top–bottom asymmetric as G is increased, until eventually our numerical solution method becomes unstable. It is hoped that these predictions might be verified, e.g., in microgravity experiments.

In all cases there is a fairly sharp transition between the conventional film and the PB, marked by an abrupt change in the first derivative of the film profile: this lends support to the simplified picture of a whole film as consisting of conventional film plus PBs (see figure 1(d)). It does *not*, however, allow an unambiguous definition of the contact angle between conventional film and PB, as the transition from one to the other is still continuous. We might adopt the heuristic definition that this transition occurs at a maximum of $\ddot{X}$, corresponding to the very large increase in $\dot{X}$ on leaving the central, nearly flat, region of the films. Alternatively,

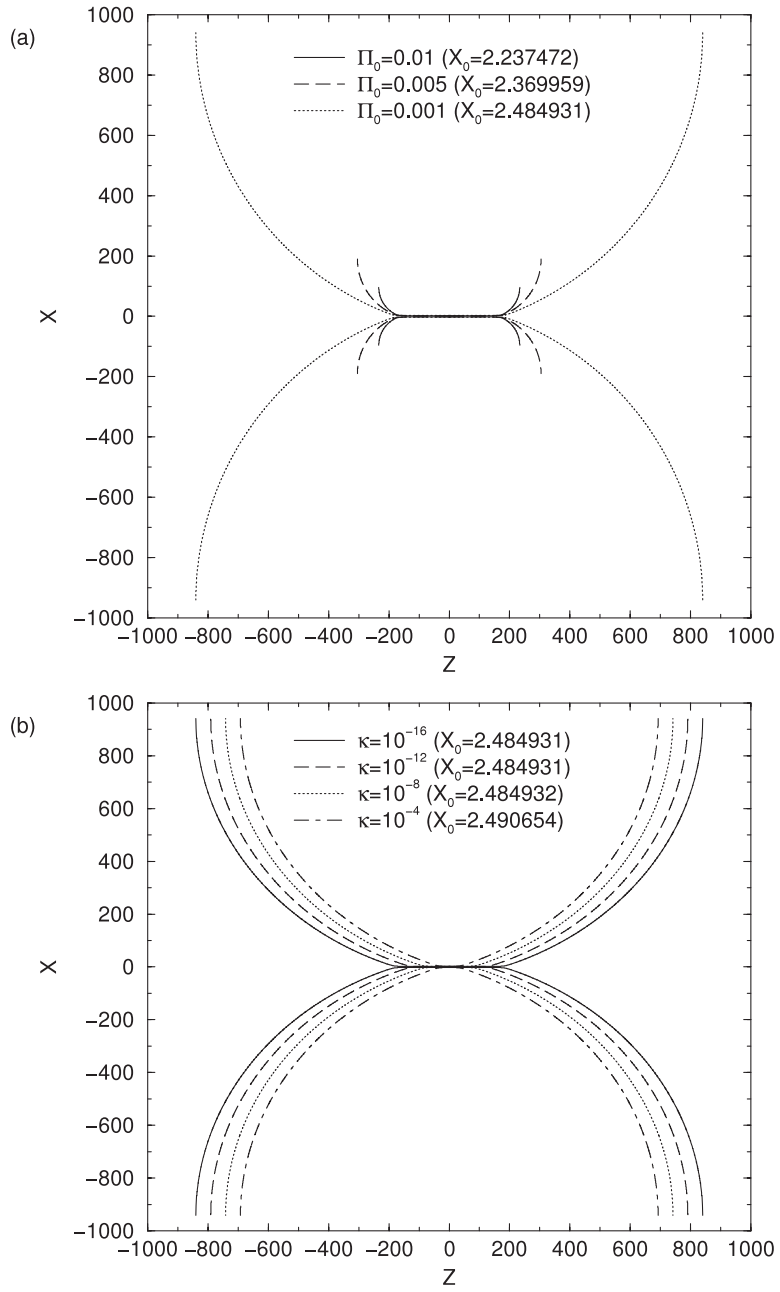

Figure 3. Film profiles in the absence of gravity ($G = 0$). (a) $\kappa = 10^{-16}$ and varying Π_0; (b) $\Pi_0 = 0.001$ and varying κ. All profiles terminate at $\theta = \pi/2$ (completely wettable bounding surfaces). The different thicknesses of the conventional films are not visible on this scale.

we could take it to be where the first (curvature) and the second (disjoining pressure) terms on the left-hand side of equation (7) are of equal magnitude, as proposed by Starov [1]. Here we do not pursue this important matter further, deferring it instead to future work.

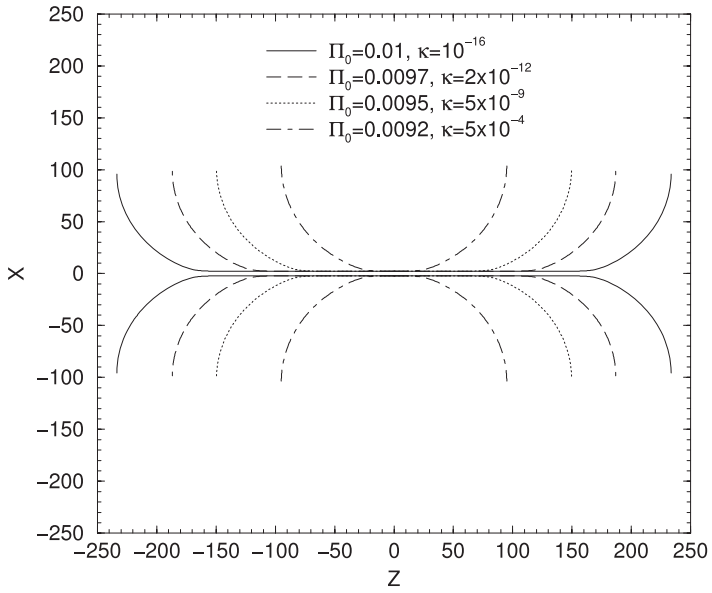

Figure 4. Films of constant volume, as might be obtained by varying the plate separation. A doubling (or halving) of the film height increases (decreases) the liquid underpressure by only about 10%. As expected, X_0 also changes slightly.

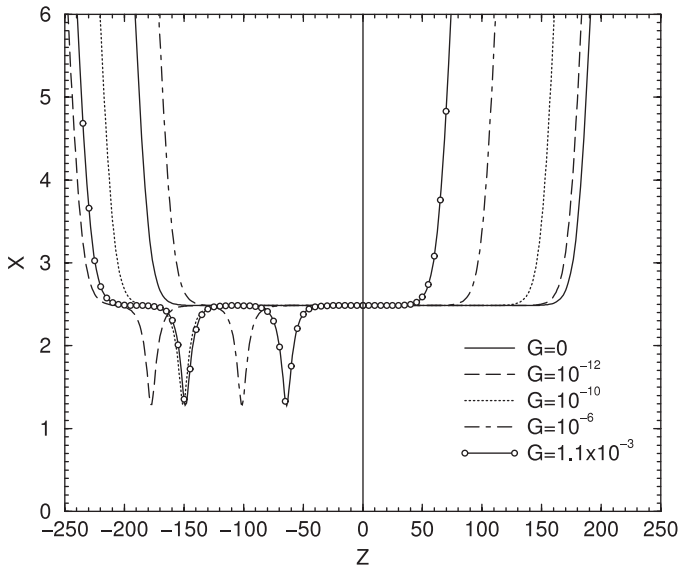

Figure 5. Effect of gravity on vertical film profiles, for $\Pi_0 = 0.001$ and $\kappa = 10^{-16}$ (for clarity only one of the surfaces of the film is shown), calculated using potential A in table 1. As the strength of gravity as measured by G increases, the films become asymmetric, their bottom (left in plot) portions increasing in length at the expense of the top (right in plot) ones. For $G \gtrsim G^* = 3.33 \times 10^{-13}$ (corresponding to $g \sim 0.4$ m s^{-2}), the lower portion of the film develops a dip: if G is further increased, then the bottom portion of the film shrinks, until for $G \sim 1.1 \times 10^{-3}$ a second dip appears. Above $G \sim 1.14 \times 10^{-3}$, the film becomes very asymmetric, with a large number of dips in its bottom portion, until for $G \gtrsim 1.19 \times 10^{-3}$ the numerical solution becomes unreliable.

All the above results were obtained for X_0 close to, and to the left of, the *second* minimum of a $\Gamma(X)$ with two minima (which is of course equivalent to having just one minimum). Clearly the discussion also applies when $\Gamma(X)$ has n minima and X_0 is located close to, and to the left of, the nth minimum. In the next section we discuss the case where X_0 is located close to, and to the left of, the *first* minimum of such a potential.

5. Film shape pathologies

The gravity-free films discussed up till now exhibit neither inflection points (where $\ddot{X}(Z) = 0$) nor stationary points (where $\dot{X}(Z) = 0$). Inspection of equation (15) with $G = 0$ and $\cos\theta$ related to $\dot{X}$ by equation (9) does not, however, rule out inflection points. At the neck (where $X = X_0$ and $\cos\theta = 1$), $\ddot{X} > 0$. As Z increases away from zero, the film thickness and slope increase, hence $\Pi(X)$ increases and $\cos\theta$ decreases. The product $\Pi(X)\cos\theta$ may then either increase or decrease. If the former, then an inflection point may be reached; this must be followed by a second inflection point at larger Z, so that the film turns upwards to match the correct PB shape. An example of this feature, which we call a *hump*, is shown in figure 6(a): in order to trigger it, $\mathrm{d}\Pi/\mathrm{d}X$ must be positive and large. Films with more than one hump are also possible in principle, but we have not been able to produce any.

If, after the first inflection point, $\cos\theta$ reaches unity, then X has a maximum. Because the film must be matched to a PB, this maximum must be followed by a minimum, which we call a *dip*. We searched for dips using the piecewise parabolic potential of figure 6(b), which allows us easily to vary the steepness and curvature of its minimum and maximum. No dips were found for gravity-free films; if, however, $G \neq 0$, equation (15) predicts that $\ddot{X} = 0$ for a sufficiently large negative Z. As noted in the caption of figure 5 (results for potential A in table 1), dips are only obtained for G greater than a threshold G^*. As G is increased above G^*, the number of dips increases, but their shape remains essentially unaltered. Further analysis is needed to establish the conditions under which humps and dips may occur and their possible effect on film stability.

One might reasonably ask how the above features are modified by thermal fluctuations of the film surfaces, hitherto neglected. To estimate the magnitude of this effect, we note that the mean square amplitude of capillary waves on a liquid–vapour interface of tension γ_L is, in zero gravity [12],

$$\langle |h(\mathbf{R})|^2 \rangle = \frac{k_\mathrm{B}T}{2\pi\gamma_\mathrm{L}} \log\frac{L}{\lambda}, \tag{18}$$

where k_B is Boltzmann's constant, T is the temperature, λ is the interfacial width and L is the (macroscopic) system size; in non-zero gravity, L should be replaced by the capillary length c, given by the fifth of equations (14). Taking $T \sim 300$ K, $\gamma_\mathrm{L} = 20$ mJ m^{-2}, $\lambda \sim 1$ nm, $L \sim 1$ cm, $c \sim 1$ mm, equation (18) yields a typical normal interface displacement $\sqrt{\langle |h(\mathbf{R})|^2 \rangle} \sim 0.7$ nm. This is about one-fifth of the thickness of a Newton black film, but only 2% of the thickness of a common black film, so there is some hope that such dips as illustrated in figure 5 might be observable in the latter system at room temperature.

6. Asymptotic solution for a thin-film profile

In this section we obtain an approximate solution to equation (15) for the conventional film. We start by approximating $\Gamma(X)$ by a truncated power expansion around $X = X_0$:

$$\Gamma(X) \approx \Gamma(X_0) + \left(\frac{\mathrm{d}\Gamma}{\mathrm{d}X}\right)_{X_0} (X - X_0) + \frac{1}{2}\left(\frac{\mathrm{d}^2\Gamma}{\mathrm{d}X^2}\right)_{X_0} (X - X_0)^2. \tag{19}$$

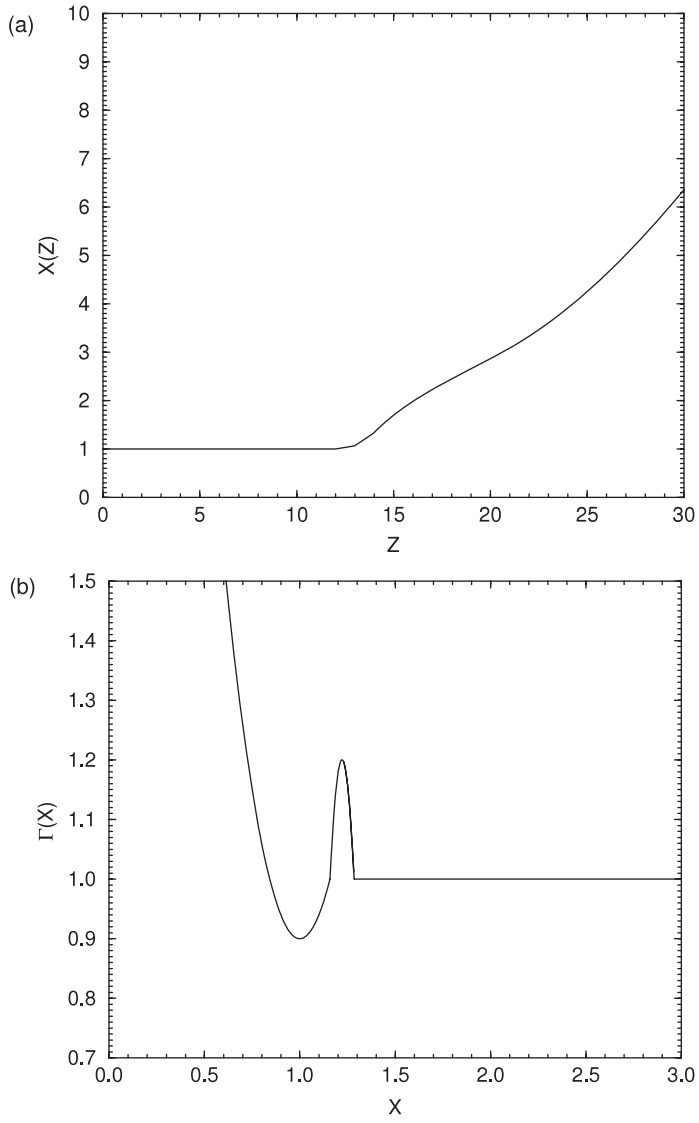

Figure 6. (a) Example of a hump obtained using potential B in table 1, for $\Pi_0 = 0.005$ and $\kappa = 10^{-16}$; the horizontal and vertical scales are different for clarity. (b) Piecewise parabolic potential used in the search for humps and dips: it has a minimum at $X = X_1 = 1$ and a maximum at $X = X_2 \approx 1.2$.

On further taking $\Gamma(X)\cos^3\theta \approx \Gamma(X_0)$ ($\theta \approx 0$, i.e., $\dot{X} \approx 0$), equation (15) simplifies to

$$\ddot{X} = \frac{1}{\Gamma(X_0)}\left[\Pi_0 + GZ + \left(\frac{\mathrm{d}\Gamma}{\mathrm{d}X}\right)_{X_0} + \left(\frac{\mathrm{d}^2\Gamma}{\mathrm{d}X^2}\right)_{X_0}(X - X_0)\right]. \tag{20}$$

The solution of this equation satisfying the boundary conditions $X = X_0$ and $\dot{X} = 0$ at $Z = 0$ is

$$X - X_0 = \kappa\xi^2\left(\cosh\frac{Z}{\xi} - 1\right) + \frac{G\xi^3}{\Gamma(X_0)}\left(\sinh\frac{Z}{\xi} - \frac{Z}{\xi}\right), \tag{21}$$

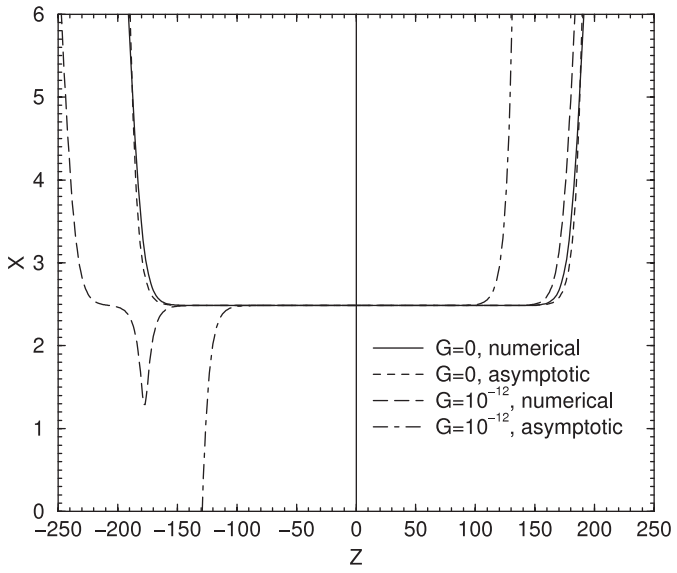

Figure 7. Comparison of numerical and analytical solutions for potential A in table 1, and $\Pi_0 = 0.001$, $\kappa = 10^{-16}$, with and without gravity. Only one half of each film is shown; they are mirror symmetric about the horizontal axis.

where κ is given by equation (17) and we have defined

$$\xi = \left[\frac{\Gamma(X_0)}{\left(\frac{\mathrm{d}^2\Gamma}{\mathrm{d}X^2}\right)_{X_0}} \right]^{1/2} . \tag{22}$$

In figure 7 we compare the asymptotic and numerical solutions, both with and without gravity: for $G > G^*$, $\ddot{X} < 0$ at the film neck and the asymptotic solution no longer yields realistic film shapes. The asymptotic and numerical profiles differ by less than 0.5% at $|Z| = 100$.

7. Summary

We have derived and solved Laplace's equation for planar soap films between two confining boundaries. We assumed that the film bounding surfaces, including their PBs, interact with a force that is perpendicular to the mid-plane of the film and depends only on film (or PB) thickness $2x$ (i.e. on the separation between bounding surfaces measured perpendicular to the mid-plane of the film). This is equivalent to a film tension $\gamma(x)$ that is a function of film thickness only, and independent of surface slope or curvature. The output is the surface profile $x(z)$ of a film with a mid-plane of mirror symmetry. We used realistic potentials (with two minima) for $\gamma(x)$ and investigated the effect of varying the film underpressure π_0, the film curvature at the neck κ, and the acceleration due to gravity g, on $x(z)$. Films with neck widths close to either of the two potential minima can then be obtained. The effect of decreasing κ is to stretch the conventional film at fairly constant PB size, whereas increasing π_0 leaves the conventional film basically unchanged and shrinks the PBs. In zero gravity, films whose minimum thickness is below the first minimum of the film tension $\gamma(x)$ may exhibit humps (two inflection points), but we have not found any dips. By contrast, under gravity we could

produce dips (i.e. thickness minima) but not humps. This of course does not mean that dips or humps are necessarily absent from either type of film, for different parameter ranges than we have explored.

Acknowledgments

We acknowledge the contributions of M E Rosa and B Saramago.

Appendix. Integration of the film profile equation

Equation (15) is equivalent to the following three equations in parametric form (where $S = s/\sigma$ is the reduced film arc length):

$$\frac{dX}{dS} = \sin\theta, \tag{A.1}$$

$$\frac{dZ}{dS} = \cos\theta, \tag{A.2}$$

$$\frac{d\theta}{dS} = \frac{1}{\Gamma(X)}\left(\Pi_0 + GZ + \cos\theta\,\frac{d\Gamma}{dX}\right), \tag{A.3}$$

where $\theta \in [-\pi/2, \pi/2]$ defines the film surface slope relative to the z-axis (see figure 1(a)). For given $\Gamma(X)$, Π_0 and G, integration starts at the neck ($S = 0$) with $Z = 0$, $\theta = 0$ and a given X_0 satisfying the inequality

$$\kappa = \frac{\Pi_0 - \Pi(X_0)}{\Gamma(X_0)} > 0, \tag{A.4}$$

and ends at the point where $\theta = \pi/2$ (for a film wetting a plate or terminating at a liquid pool; see figures 1(a) or (b)) or $\theta = \pi/6$ (for three identical films meeting, see figure 2(a)).

In equation (A.4), κ is the film curvature at the film neck: flat films are obtained for $\kappa \ll 1$. In zero gravity, $G = 0$ and the film is symmetrical ($X(Z) = X(-Z)$). In non-zero gravity, $G \neq 0$ and the upper ($Z > 0$) and lower ($Z < 0$) film halves correspond to positive and negative values of the arc length S, respectively. Numerical solution of equations (A.1)–(A.3) was performed using variable-step-size Runge–Kutta or Bulirsch–Stoer methods [13].

References

[1] Starov V M 2004 *J. Colloid Interface Sci.* **269** 432
[2] Derjaguin B V, Churaev N V and Muller V M 1987 *Surface Forces* (New York: Plenum)
[3] Starov V M 1992 *Adv. Colloid Interface Sci.* **39** 147
[4] Israelachvili J N 1991 *Intermolecular and Surface Forces* 2nd edn (London: Academic)
[5] Bergeron V 1999 *J. Phys.: Condens. Matter* **11** R215
[6] Bergeron V and Radke C J 1992 *Langmuir* **8** 3020
[7] Theodoly O, Tan J S, Ober R, Williams C E and Bergeron V 2001 *Langmuir* **17** 4910
[8] Bergeron V and Claesson P M 2002 *Adv. Colloid Interface Sci.* **96** 1
[9] Derjaguin B V and Obuchov E 1936 *Acta Phys. URSS* **5** 1
[10] Isenberg C 1992 *The Science of Soap Films and Soap Bubbles* (New York: Dover)
[11] Fortes M A 1980 *Phys. Chem. Liq.* **9** 285
[12] See, e.g. Barrat J-L and Hansen J-P 2003 *Basic Concepts for Simple and Complex Liquids* (Cambridge: Cambridge University Press)
[13] Press W H, Teukolsky S A, Vetterling W T and Flannery B P 1992 *Numerical Recipes: The Art of Scientific Computing* 2nd edn (Cambridge: Cambridge University Press)